Tellus (1995), 47A, 656–670
Printed in Belgium – all rights reserved

TELLUS
ISSN 0280-6495

The structure and evolution of an explosive cyclone near Iceland

By JÓN EGILL KRISTJÁNSSON[1] and SIGURDUR THORSTEINSSON*, *Icelandic Meteorological Office, Bústadavegi 9, IS-150 Reykjavík, Iceland*

(Manuscript received 9 September 1994; in final form 9 March 1995)

ABSTRACT

In the first study of a series of studies of intense cyclones in the active region around Iceland, the explosive synoptic-scale "Greenhouse Low" that hit Iceland on 3 February 1991 is studied. We have investigated this cyclone mainly through numerical simulations with an NWP model (HIRLAM), but also by careful reanalysis of surface observations and satellite pictures. The cyclone formed in an unusually baroclinic air mass just north of the Azores in the early hours of 2 February 1991. A baroclinic wave formed and developed, aided by latent heat release. During this period, we have found evidence of symmetric instability in a deep layer. Between 18 UTC 2 February and 06 UTC 3 February, the central pressure fell by more than 30 hPa, as the cyclone deepening continued. Over the next 6 h, a further deepening of 15 hPa occurred, as an upper level potential vorticity anomaly caught up with and reinforced the cyclone. At this time, hurricane-force winds were observed at numerous sites in the southern and western parts of Iceland, with mean winds up to 57 m s^{-1}. As the cyclone continued its northward movement, a pressure rise of 30.4 hPa in 3 h was recorded at one station. Reruns with the HIRLAM model, using ECMWF analyses from 12 UTC 2 February as initial conditions, captured all the main features of the observed development, helping us to draw the above picture. Corresponding runs from 00 and 06 UTC had considerable errors in both positioning and deepening of the storm. The sensitivity of the simulations to the removal of surface energy fluxes and latent heat of condensation was investigated separately. It was found that over the time span of the simulation, surface energy fluxes had negligible impact on the explosive development. The contribution of latent heat release to the development appears to be about half that of dry baroclinic instability. These findings are discussed in view of related studies in the literature.

1. Introduction

The "Icelandic low" is a well-known feature of the general circulation of the Northern Hemisphere. It is characterized by a semi-permanent surface low SW of Iceland, clearly visible in monthly or seasonally (winter) averaged fields (e.g., Wallace and Hobbs, 1977). In wintertime, in particular, the region around Iceland is an area of great baroclinic activity, ranging from small-scale polar lows to large-scale cyclonic vortices (see Fig. 13.6.2. in Petterssen, 1956). The most important meteorological features of this region are: (i) the vicinity of the semi-permanent "polar front", (ii) the warm North Atlantic ocean current (the "Gulf Stream") which enhances the temperature gradients vis-à-vis the Arctic, and at the same time yields a large flux of heat and humidity into the air, which is usually colder than the sea surface (Stefánsson, 1960), (iii) the proximity of Greenland, which in addition to serving as a huge cold reservoir, has also, due to its height, size and shape, a very strong influence on the large-scale flow (Shapiro, 1985).

[1] Permanent affiliation: Institute of Geophysics, University of Oslo, P.O. Box 1022 Blindern, 0315 Oslo, Norway.
* Corresponding author.

This study is the first in a series of studies with the purpose of better understanding the roles of physical, dynamic, and topographic factors in determining the behaviour of intense cyclones near Iceland. Different types of cyclones will be treated in the series of studies.

In this paper, an explosive synoptic-scale cyclone that developed near the Azores Islands has been investigated. The cyclone hit Iceland on 3 February 1991 and derives its name ("Greenhouse Low") from the extensive damage it caused to greenhouses in southern Iceland. Although not exceptionally deep, this storm was one of the most devastating cyclones to hit Iceland this century. This is due to the enormous pressure gradients associated with it as well as the cyclone track, which caused the area of strongest winds on its eastern side to hit the most populated areas hardest.

Over the last 10–15 years, many studies have been published, investigating explosive synoptic-scale cyclones in different parts of the world. In particular, interest has focused around cyclones forming off the east coast of North America (e.g., Gyakum, 1983; Uccellini, 1990), as well as those hitting Great Britain and France (e.g., Hoskins and Berrisford, 1988; Shutts, 1990). In this study we shift the focus to the stormy region around Iceland. As we progress, we will relate our findings to these studies, highlighting both similarities and differences.

Most of these studies have employed numerical weather prediction (NWP) models, both to diagnose essential features of the cyclones, as well as to quantify the role of different processes in their evolution. This method is also adopted here. The objectives of this investigation are:

1. to document the three-dimensional structure and evolution of the cyclone.
2. to investigate the causes of the rapid development.
3. to identify some characteristics of explosive cyclones near Iceland.

In Section 2, we describe the synoptic weather maps and synoptic observations from Iceland during the passage of the Greenhouse Low. This is followed by numerical simulations in Section 3. Section 4 contains a summary of the results in the previous sections and relates our findings to those of other studies.

2. Synoptic description of the explosive cyclone 2–3 February 1991

As pointed out by Gíslason (1991), the atmosphere over the North Atlantic was unusually baroclinic on 2 February 1991, partly as a result of "pre-conditioning" in the preceding days. This preconditioning was created by several deep cyclones that moved up to southern Greenland and advected very cold air southward and southeastward over the Atlantic. At the same time there was a blocking high over Northern Europe which provided mild air from a southerly direction into the eastern part of the North Atlantic. According to Vautard's (1990) classification this is a typical case of the "European blocking pattern". This blocking undoubtedly serves to enhance the baroclinicity in the Atlantic as it impedes the eastward progression of the cold air.

The baroclinicity is revealed by Fig. 1, showing analyzed 500 hPa height and 1000–500 hPa thickness at 12 UTC 2 February 1991. For instance the thickness gradient across this baroclinic zone between 50.5° N, 38.0° W and 46.5° N, 31.5° W corresponds to a thermal wind of 64 m s^{-1} (124 knots) from the southwest. Just at the warm edge of this baroclinic zone the surface analysis identified an open baroclinic wave (Fig. 2a) with a central pressure of $\approx$997 hPa, according to

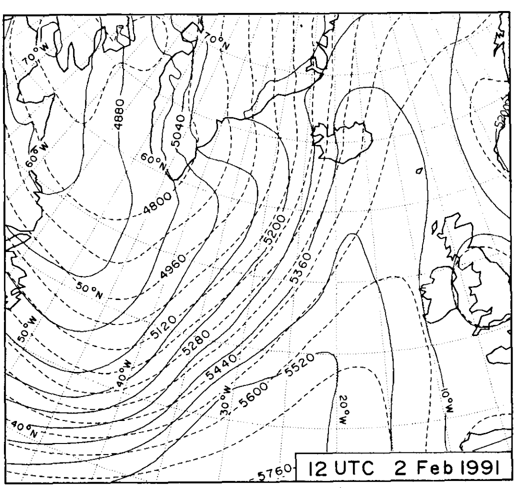

Fig. 1. ECMWF analysis of 500 hPa geopotential height (solid) and 1000–500 hPa thickness (dashed) at 12 UTC 2 February 1991.

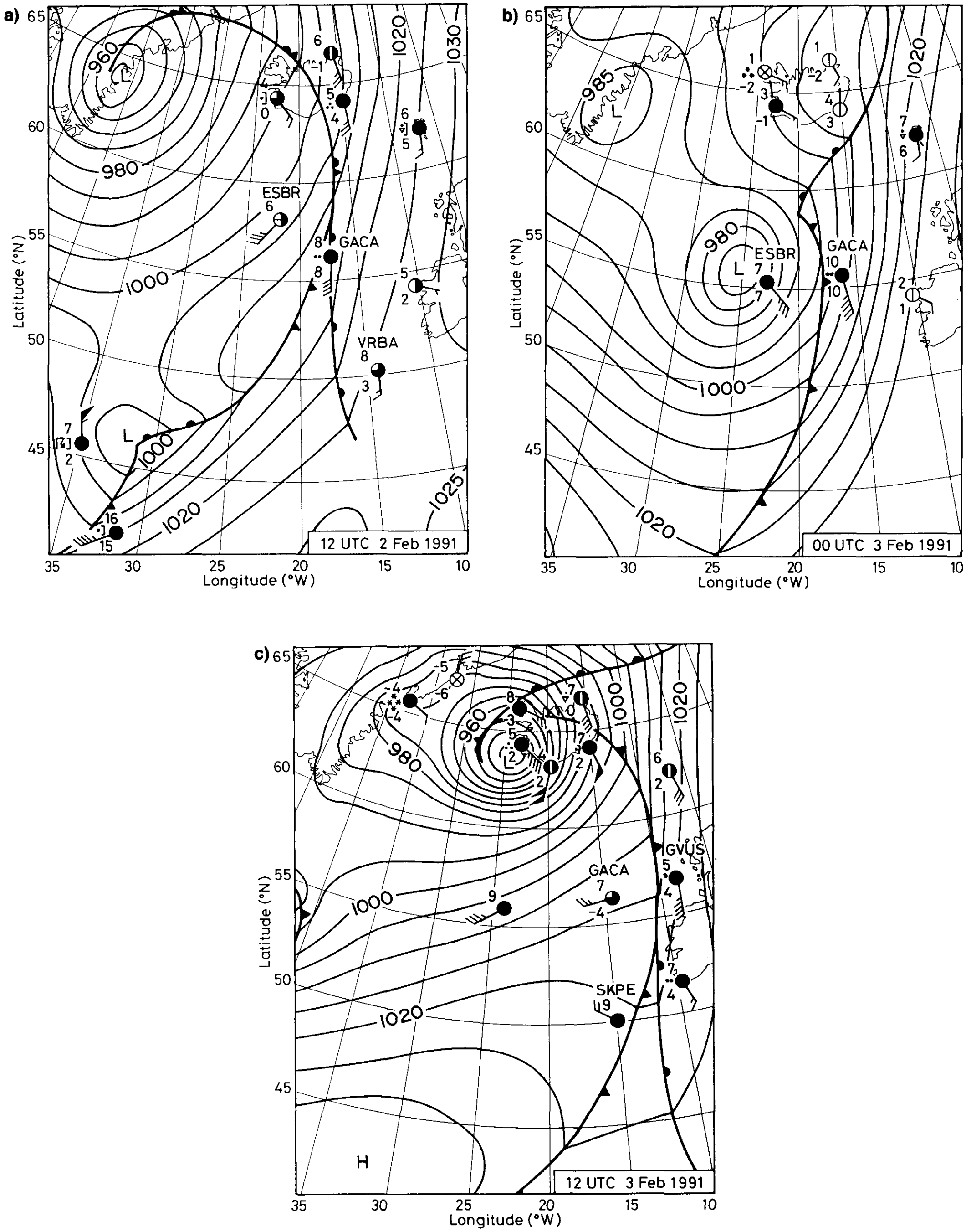

Fig. 2. Subjective analysis of sea level pressure and fronts at: (a) 12 UTC 2 February 1991; (b) 00 UTC 3 February 1991; (c) 12 UTC 3 February 1991. Ships, buoy and coastal observations include air temperature and dew point (°C), wind vectors (one full barb = 5.2 m s^{-1}, one pennant = 25.9 m s^{-1}), and weather, plotted according to standard conventions.

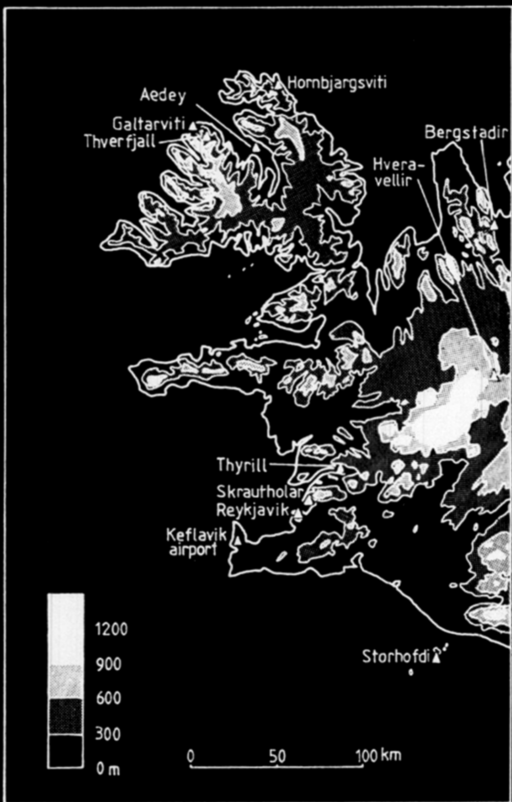

Fig. 3. Shown are some of the weather stations in the western part of Iceland (see Table 1). Shading indicates topographic height in meters.

our analysis. Only 24 h later, the low centre was at 63.5° N, 24° W (Fig. 2c). By then it had deepened by approximately 55 hPa, placing it in the category of unusually rapidly deepening cyclones (Roebber, 1989). The deepening was fairly steady around 14 hPa/6 h during this 24-h period, but different mechanisms contributed at different times, as will be explained in Subsection 3.2.

Between 12 and 18 UTC on 3 February, the cyclone was in its most intense phase and causing extensive damage. The pressure gradient around the centre was exceptionally steep and a remarkable surface pressure tendency of +30.4 hPa/3 h was observed at Keflavík airport (for locations see Fig. 3) between 12 and 15 UTC. This is certainly an unusually large pressure rise for an extratropical cyclone. We have found two examples of larger pressure tendencies in the literature and

Table 1. *Maximum wind speeds measured on 3 February 1991; for locations see Fig. 3 (note that the upper limit of the wind recorder is 61.8 m s^{-1} (120 knots); this limit was evidently exceeded at Stórhöfdi and Thyrill)*

Stations	Height above sea level (m)	Max. 10 min. mean wind speed (m s^{-1})	Max. wind gust (m s^{-1})
Stórhöfdi	118	56.6	>61.8
Keflavík Airport	49	34.5	46.3
Reykjavík Met. Office	52	32.9	41.2
Reykjavík Airport	14	35.0	40.6
Thyrill	53	43.8	>61.8
Hveravellir	641	43.2	52.5
Skrauthólar	30	34.0	56.1
Thverfjall	752	36.0	54.0
Galtarviti	20	37.1	—
Ædey	5	39.1	52.5
Hornbjargsviti	27	34.0	52.0
Bergstadir	43	35.0	—

both refer to Atlantic cyclones: Tryggvason (1960) reported an observed pressure rise of +33 hPa/3 h at Dalatangi on the east coast of Iceland in January 1949, while an even larger pressure tendency of −35.0 hPa/3 h was reported by Stubbs (1975) at 44° N, 41° W in September 1972, followed by a pressure rise of +32.5 hPa/3 h.

Many stations over the whole western part of Iceland observed hurricane force surface winds (Table 1): Stórhöfdi on the Westman Islands off the south coast reported a mean wind of 56.6 m s^{-1} (110 knots). This is the strongest wind ever measured in Iceland and probably among the strongest winds ever measured outside the tropics, with the obvious exception of high mountains. In the case referred to by Stubbs (1975), the strongest mean wind was 43.7 m s^{-1} (85 knots).

3. Numerical simulations

We shall now look at operational NWP model simulations as well as sensitivity runs that have been conducted to better understand the role of different meteorological factors in the simulations of the low.

Table 2. *Surface pressure (hPa) at different times from simulations and subjective analysis (ANALYS)*

Runs	2/00 (hPa)	2/06 (hPa)	2/12 (hPa)	2/18 (hPa)	3/00 (hPa)	3/06 (hPa)	3/12 (hPa)	3/18 (hPa)	4/00 (hPa)
ANALYS			997		971	957	942		
CONTROL			1002	988	972	956	943	939	956
NOLAT			1002	994	985	973	963		
NOPHYS			1002	990	974	952	932		
RUN-00	1015	1010	1005	996	986	975	967		
RUN-06		1012	1001	989	975	964	953		

3.1. Operational model runs

The operational weather prediction models at the time had varying degrees of success in predicting this event. The European Centre for Medium Range Weather Forecasts' (ECMWF) +24 h prediction from 12 UTC on 2 February was fairly successful, deepening the low to 954 hPa (i.e., underestimating it by 12 hPa; Table 2), but placing it slightly too far north. Earlier predictions from ECMWF and the United Kingdom Meteorological Office (UKMO), however, failed to predict both the position and intensity of the low. For instance, the UKMO fine mesh prediction from 12 UTC 2 February gave a central pressure of about 969 hPa and a position some 200 km too far east. Apparently, the High-Resolution Limited Area Model (HIRLAM), operational in Denmark at the time, suffered from the same problem in this case, as discussed by Gíslason (1991). Since the UKMO fine-mesh model has an earlier "cut-off" than ECMWF in its data assimilation, it seems likely that the ECMWF analysis at 1200 UTC on 2 February contained some additional observations which turned out to be important for the development of the storm during the first hours. According to Norris and Young (1991), subsequent runs of the operational UKMO model based on an analysis enhanced by use of satellite data gave a radically improved simulation of the development.

3.2. The CONTROL run and the role of symmetric instability

In this study HIRLAM has been run, using ECMWF analyses, interpolated to the HIRLAM grid as initial and boundary values. The model was integrated on a transformed latitude-longitude grid with a horizontal resolution of 0.5° corresponding to about 56 km. There are 16 levels in the vertical, where a hybrid coordinate (cf. Simmons and Burridge, 1981) is used. This coordinate approaches "p" as the pressure tends to zero but approaches "sigma" as the pressure tends to the surface pressure. The forecast system is a comprehensive numerical weather prediction system developed in a joint research project between the Nordic countries, the Netherlands and Ireland. Recent developments and upgrading of the system are described by Gustafsson (1993).

The simulation starting at 12 UTC 2 February, using the standard version of the HIRLAM model, as of early 1992 ("HIRLAM 2"), will hereafter be termed CONTROL run. From this run, sea level pressure and 850 hPa equivalent potential temperature are shown in Figs. 4a–b at 12 hourly intervals. All the main features shown in Fig. 2 were captured by this simulation, so we will look here only at the intermediate times. First at 18 UTC on 2 February (Fig. 4a), we see how the baroclinic wave 6 h earlier (Fig. 2a) has developed into a closed 988 hPa low. The gradient in equivalent potential temperature on the "cold side" of the low is very tight, indicating the sharp contrast between the two air masses. 12 h later, at 06 UTC on 3 February the low has deepened by 32 hPa and moved about 1200 km northwards (Fig. 4b). Note how the θ_e-lines are "sucked in" towards the low pressure center, visualizing the role of the warm conveyor belt ahead of the cold front. Referring to the Norwegian cyclone model, the warm sector has become quite narrow now, suggesting that the cyclone may soon exhaust its energy supply. The depression then goes on deepening to 939 hPa at 18 UTC (Fig. 5), but after that starts filling as it enters Greenland and has a central pressure of 956 hPa at 00 UTC on 4 February (Table 2).

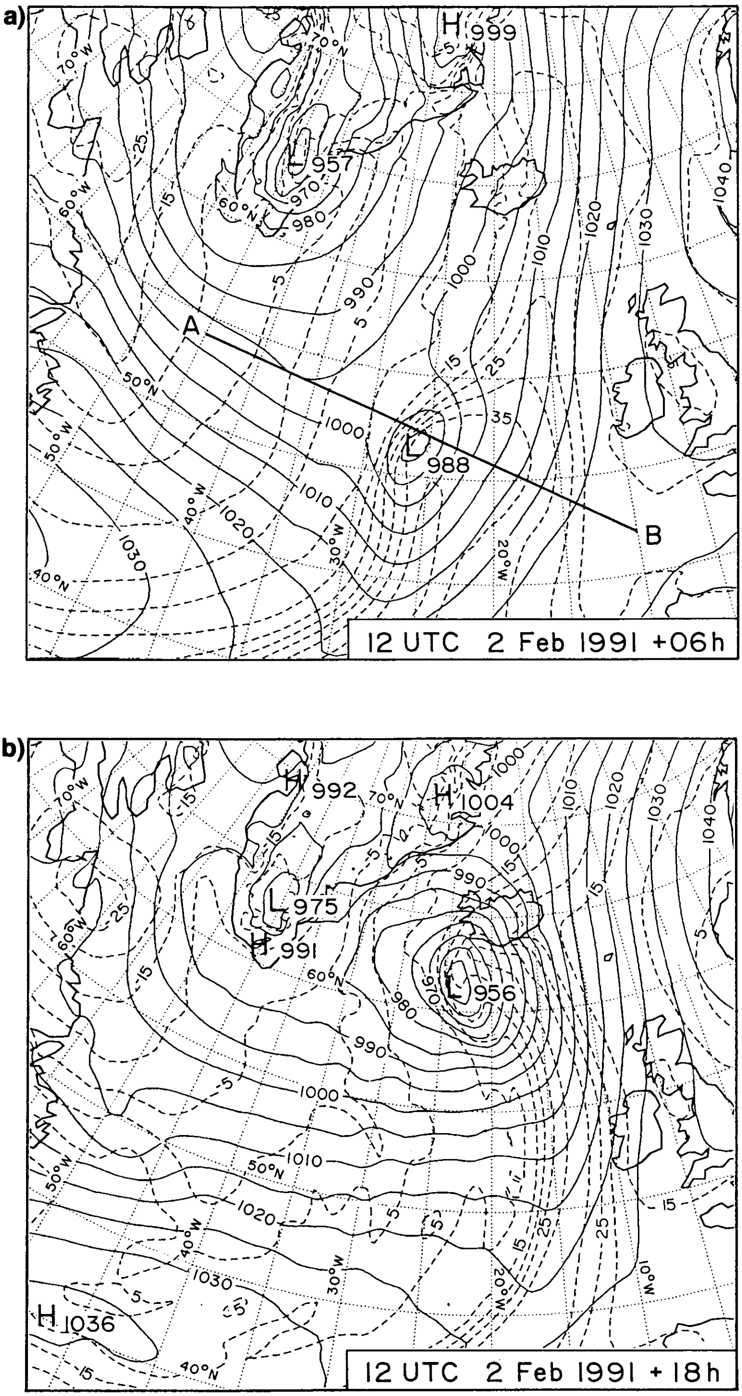

Fig. 4. Surface pressure (hPa) and 850 hPa equivalent potential temperature (°C, dashed) in CONTROL run: (a) 18 UTC 2 February 1991; (b) 06 UTC 3 February 1991.

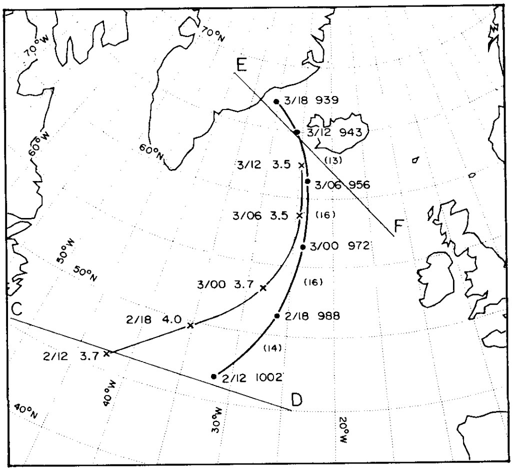

Fig. 5. Storm tracks from CONTROL run. Bold line: Surface cyclone position (dots, every 6 h) and central pressure (hPa); numbers in parentheses are surface pressure deepenings over 6 h. Thin line: 300–500 hPa maximum potential vorticity (x, PVU).

Further insight is gained from the satellite picture at an early stage in the cyclone development (Fig. 6). As pointed out by Norris and Young (1991) it has several interesting features. The main features are the front oriented SW–NE with what appears to be a growing wave on it, and the huge cloud system west of this front (cloud head), which Norris and Young (1991) suggest is caused by extensive slantwise ascent. It seems plausible to attribute the cloud head to the secondary low centre indicated in Fig. 2b, southwest of the frontal wave. Later (Figs. 2c, 4b) these two systems gradually merge together, as suggested by satellite imagery (Gíslason, 1991) and PV considerations; see Subsection 3.3.

Fig. 7a shows a vertical cross-section through the center of the storm at 18 UTC, i.e., at an early stage in the cyclone development. The end points of the section are indicated in Fig. 4a. Areas with more than 90% relative humidity are shaded. We immediately recognize several features that were seen in Fig. 6, e.g., the frontal clouds beneath the high tropopause in the warm air to the right of the figure. To the left of that there is a "dry intrusion" (Norris and Young, 1991), and then the above mentioned cloud head. By following a line for constant absolute momentum per unit mass, $M = fx + v_g$, within the shaded region we can evaluate the potential for slantwise convection. The x-axis lies along the cross-section. Choosing the line $M = 156$ m s^{-1}, we find that θ_e drops from 26°C at 1000 hPa to 18°C at 500 hPa, indicating a fairly large symmetric instability along the M-surface. This supports the above interpretation of the satellite picture, and suggests that slantwise convection may have played an important role by releasing energy in the central portions of the low during its developing stage. A similar result was found by Shutts (1990) for the "October storm" that hit Great Britain in 1987.

3.3. *Potential vorticity diagnostics based on CONTROL run*

Following the comprehensive paper by Hoskins et al. (1985), there has in recent years been a growing interest in the role of potential vorticity (PV) anomalies in connection with cyclone deepening. These can be, e.g., upper level anomalies originating in the stratosphere or lower level anomalies produced by diabatic heating. We have looked at the evolution of PV for all the runs for the 3 layers 500–300 hPa, 700–500 hPa and 850–700 hPa. The geographical relationship of the surface low, the 500–300 hPa PV anomaly, and 6-hourly pressure falls is seen in Fig. 5.

Starting with the lower troposphere, the PV field at 850–700 hPa from the CONTROL run shows a well-organized maximum in PV along the front, near the cyclone center. It reaches 3 PVU (1 PVU $= 10^{-6}$ kg^{-1} m^2 s^{-1} K) already after 12 h and about 3.5 PVU at +18 h (Fig. 8). This anomaly is most likely caused by latent heat release, in accordance with the findings of Shapiro and Keyser (1990) and Shutts (1990). We shall return to the role of latent heat in the next subsection. Higher up we find for 700–500 hPa that the PV-field has a band of high values in the cold air extending from the cyclone center (not shown), where the highest values of about 2.7 units are found at +12 and +18 h.

At upper levels, i.e., in the 500–300 hPa layer, there is to begin with a zone of positive PV values of up to 4 PVU, located about 850 km to the west of the cyclone (Fig. 5). This zone approaches the surface cyclone and by +12 h probably starts interacting with it, yielding the mutual coupling discussed by Hoskins et al. (1985), finally resulting in the merging discussed in Subsection 3.2. This

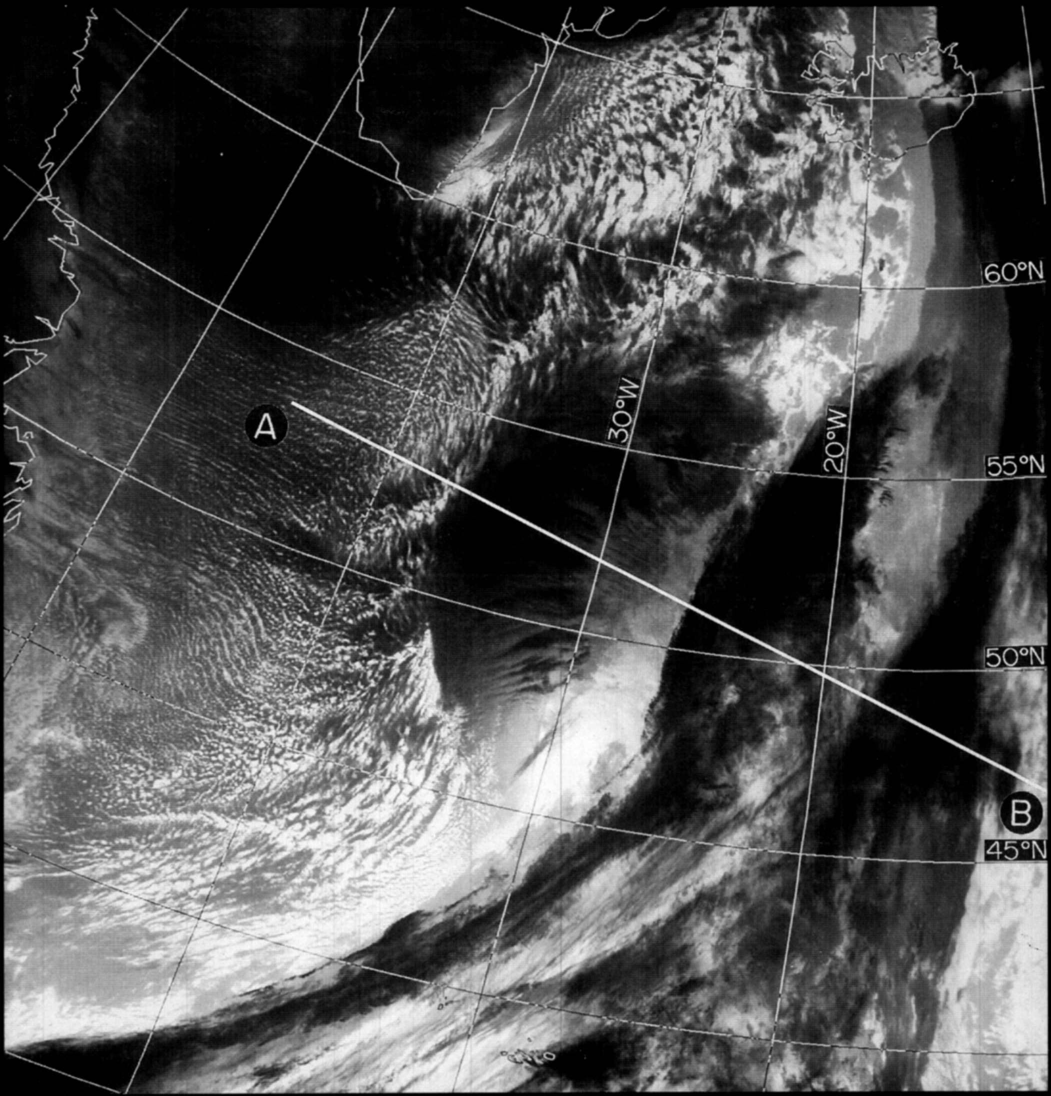

Fig. 6. Infrared satellite picture from 1550 UTC 2 February 1991 (Courtesy of University of Dundee).

merging is supported by the PV cross sections shown in Figs. 9a, b. In Fig. 9a the low-level PV anomaly is weak while an upper-level anomaly can be identified farther west. Twenty four hours later, as shown in Fig. 9b, the two anomalies are coupled together in a similar way as was shown by Uccellini (1990) for the Presidents' Day storm. This figure is taken from the analysis data, which confirms that the proposed coupling is not merely an artifact of the CONTROL simulation. The corresponding figure from CONTROL (not shown) is very similar, except the PV anomalies are somewhat stronger.

3.4. *Sensitivity experiments*

The results of additional simulations with HIRLAM provide some insight into the sensitivity of the CONTROL simulation to the treatment of:

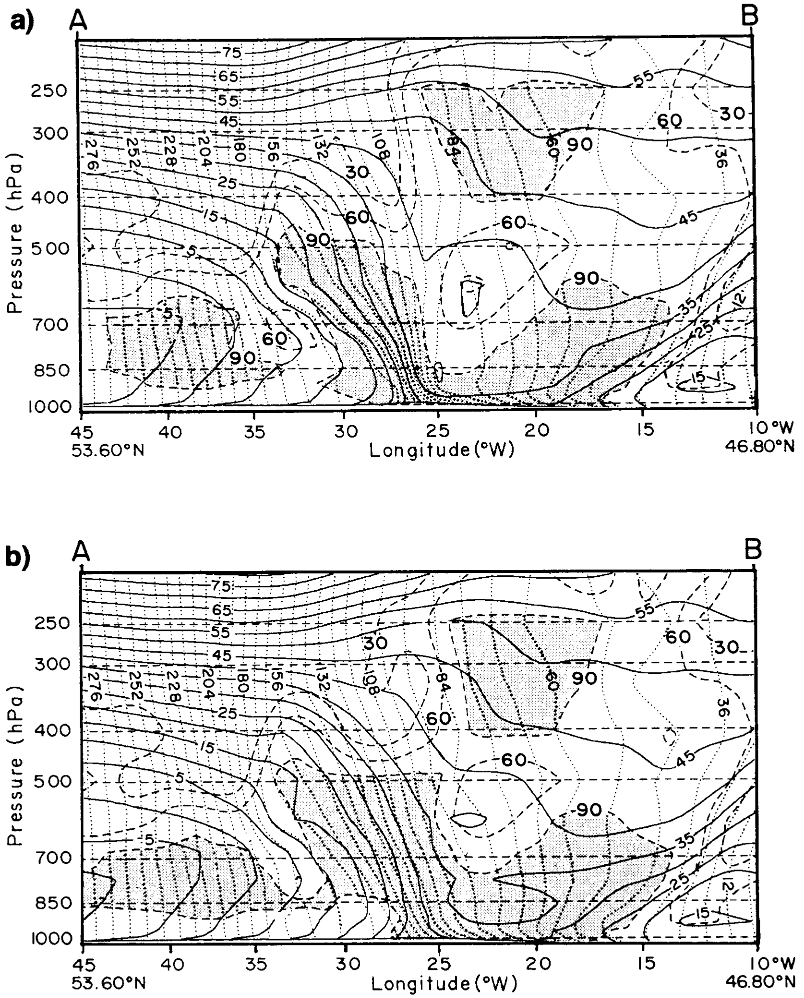

Fig. 7. Cross-section from A to B in Fig. 4a, displaying equivalent potential temperature (solid, °C), absolute momentum per unit mass (dotted, m s^{-1}) and relative humidity (dashed, %) at 1800 UTC 2 February: (a) CONTROL, (b) NOLAT.

(A) latent heat, (B) model physics, (C) boundary layer processes, (D) topography. We have examined A and B by conducting runs without latent heating and without accounting for the physical processes, respectively. Topic C consisted of running the model without turbulent fluxes from the surface, while D was investigated by reanalyzing and then rerunning the model without the Greenland orography.

3.4.1. Effect of latent heat (NOLAT). The central pressure at 1200 UTC on 3 February in a simulation where latent heat was omitted was 20 hPa higher than in the control run, while the position of the low was little affected (see Tables 2, 3). Hence, the latent heat contributes about 1/3 of the rapid deepening of the low. Many other studies of explosive cyclogenesis have found the latent heat to be responsible for at least half the deepening (e.g., Kuo and Reed, 1988; Reed et al., 1992). In their investigation of three explosive North Atlantic cyclones, Reed et al. (1988) found latent heating to be responsible for about 40–50%

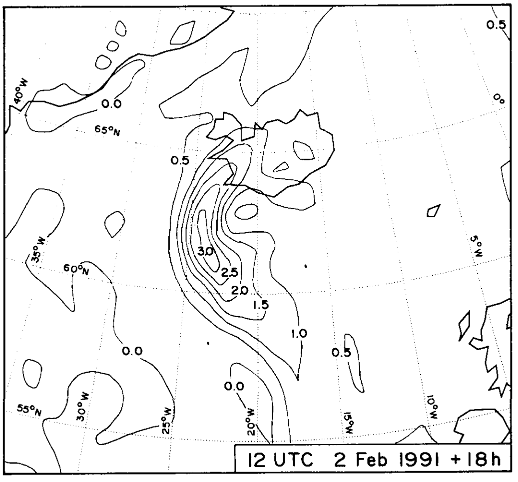

Fig. 8. Potential vorticity (units: PVU $= 10^{-6}$ kg^{-1} m^2 s^{-1} K) at 700–850 hPa at 06 UTC 3 February 1991 from CONTROL.

of the deepening. In the case of another very intense cyclone in the North Atlantic in January 1992, Breivik et al. (1992) found a similar latent heating contribution to that found here. As in that case, it appears that although latent heating was important in producing low-level potential vorticity near the low center, it was the exceptionally large dry baroclinicity that was the most characteristic feature.

Fig. 7b shows a cross-section analogous to that in Fig. 7a, but now for NOLAT. The most noticeable difference is that the frontal zone, as compared to CONTROL, is much wider and has weaker gradients of θ_e and M, the latter being a measure of absolute vorticity. Also the stability is now stronger between 700 and 500 hPa. Below

Table 3. *Cyclone deepenings adjusted to 45°N as in Roebber (1989)*

Runs	24 h d.adj. (hPa)	12 h d.adj. (hPa)
CONTROL	50	27
NOLAT	33	18
NOPHYS	60	32
NOGREEN	48	26
RUN-00	31	18
RUN-06	41	21

this, however, we can follow a constant M-line ($M = 132$ m s^{-1}) within the region of greater than 90% relative humidity and find a decrease in equivalent potential temperature of only 6°C between 1000 hPa and 700 hPa. The difference between Fig. 7a, b serves to show how latent heating enhances vertical motions, leading to a narrower updraft (Emanuel, 1985), and hence helps to spin up the cyclone at low levels.

3.4.2. Effect of physical parameterizations (NOPHYS). In a simulation disregarding all physical processes (i.e., surface friction, latent heating, radiation, vertical diffusion and surface fluxes), the central pressure at +24 h was 11 hPa lower than in the CONTROL run (Table 2). Presumably this was mainly due to lack of surface friction. The position at +24 h, however, was quite similar to that observed, and hence better than in CONTROL.

The PV diagnostics reveal (not shown) that in NOPHYS, the low-level (850–700 hPa) PV maximum near the low center was considerably weaker than in CONTROL, and the secondary maximum along the front was totally absent. This is probably due to lack of PV generation through latent heat release in NOPHYS. At 500–300 hPa the PV anomaly in NOPHYS is very similar to that in CONTROL at all times. This supports the notion that the upper PV-"anomaly" is a separate feature that forces the lower level flow rather than vice versa.

3.4.3. Effect of surface fluxes (NOFLUX). A simulation where the fluxes of heat and moisture between the earth's surface and the atmosphere were set to zero was conducted and termed NOFLUX. This turned out to have a negligible impact, i.e., the cyclone deepening was almost identical to that in CONTROL. One possible explanation is that the forcing from larger scale baroclinicity and latent heating is so strong that the surface fluxes don't have time to act. Also we can visualize the following scenario: In the cold air the surface heats up the air greatly, but this would act to weaken the baroclinicity, if anything. On the warm side the air entering from southeast is probably warm enough that the heating from the surface is quite small. And it seems likely that the air already contains enough humidity from advection from lower latitudes that a large latent heat flux from the surface is not needed to maintain the latent heat release that we found. Interestingly, this

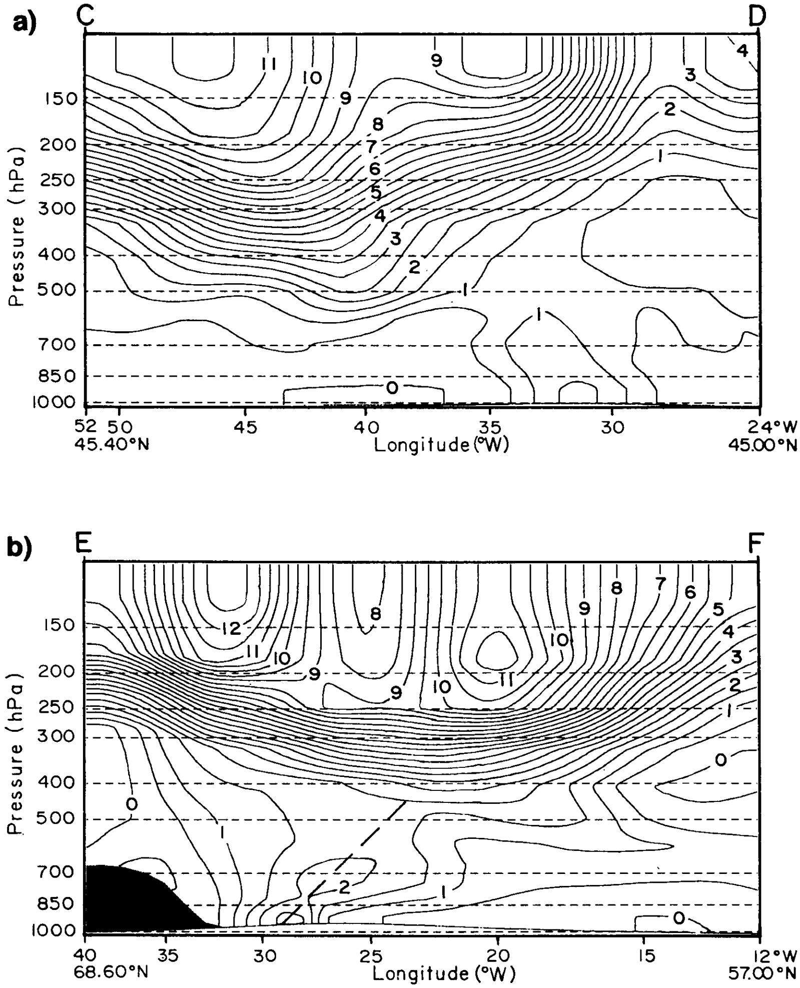

Fig. 9. Cross section of potential vorticity along lines in Fig. 5, from ANALYS: (a) line C–D at 12 UTC 2 February 1991; (b) line E–F at 12 UTC 3 February 1991. The broken line indicates the connection between the lower and upper potential vorticity anomalies.

result is quite analogous to the numerical simulations of a North Atlantic winter cyclone by Reed and Simmons (1991). Clearly, it would be of interest to see if the evaporation from the sea surface is relatively more important in the preconditioning stage. We hope to address this important issue at an appropriate time in the future.

3.4.4. Effect of Greenland (NOGREEN). To investigate the effects of the Greenland topography on the cyclone development, a reanalysis without Greenland was conducted with data from 12 UTC 2 February. This was partly motivated by the findings of Breįvik et al. (1992) that the Greenland topography had a major impact on the positioning of the low studied there, probably due to its effect on the supply of cold air from the arctic.

The reanalysis was done as follows: Surface pressure values were estimated by an integration of the hydrostatic equation from the ECMWF surface level to the HIRLAM NOGREEN surface level using a virtual temperature profile expressed as a linear function of $\log_e$(pressure) in the vicinity of the HIRLAM surface level. The model was then run for 24 h. The result (Tables 2, 3) is quite close to CONTROL, although the central pressure is 2 hPa higher and the position is about 100 km farther northeast at 12 UTC 3 February. Worth mentioning also is a pressure difference of +20 hPa between NOGREEN and CONTROL near the west coast of Greenland (68° N, 52° W), presumably due to lee effects (i.e., vortex stretching), as the wind field is southeasterly (Fig. 1). Hence, it is concluded that the Greenland topography has a large and non-trivial impact on the pressure distribution around the island, but that it had a rather small effect on the development and movement of the Greenhouse Low.

3.5. Different starting times (00 and 06 UTC 2 February)

We conducted a 36-h simulation with initial time at 00 UTC 2 February and termed it RUN00. This simulation gave nearly the same result as most of the operational forecasts at the time, i.e., it failed to show the explosive development of the low and, furthermore, displaced the low by about 200 km eastward at +36 h. The pressure error in the centre of the low at 1200 UTC on 3 February was 25 hPa, giving only 967 hPa at +36 h, as compared to 943 hPa from CONTROL (see Table 2). We believe that finding out why RUN00 fails may also help explain why the operational model forecasts were so inaccurate.

From Table 2, we see how the low center in RUN00 is 3 hPa weaker than in CONTROL already at 12 UTC 2 February. The difference then increases at a fairly even rate of 5–6 hPa/6 h over the next 24 h. We have tried to understand this large difference by studying the differences between the model fields in the two runs before the explosive development took place, i.e., at 12 UTC 2 February. Some differences were found in the humidity fields, suggesting that missing humidity data may have played a role. This also lends some support from the interesting similarity between the surface pressure evolution in runs RUN00 and NOLAT, seen in Table 2. But the most prominent difference was found in the temperature field in the mid to lower troposphere, as shown in Fig. 10.

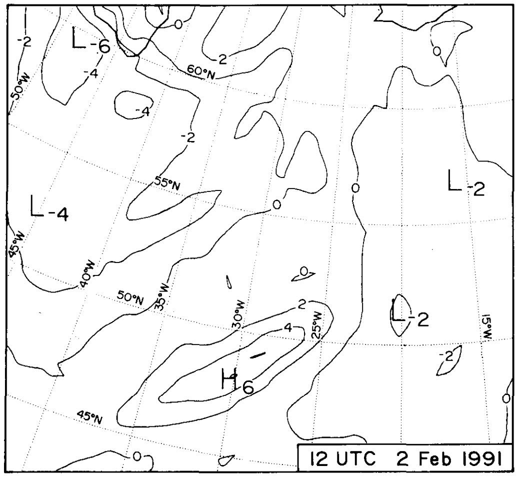

Fig. 10. Temperature difference between CONTROL and RUN-00 at model level 12 (approximately 820 hPa) at 12 UTC 2 February 1991.

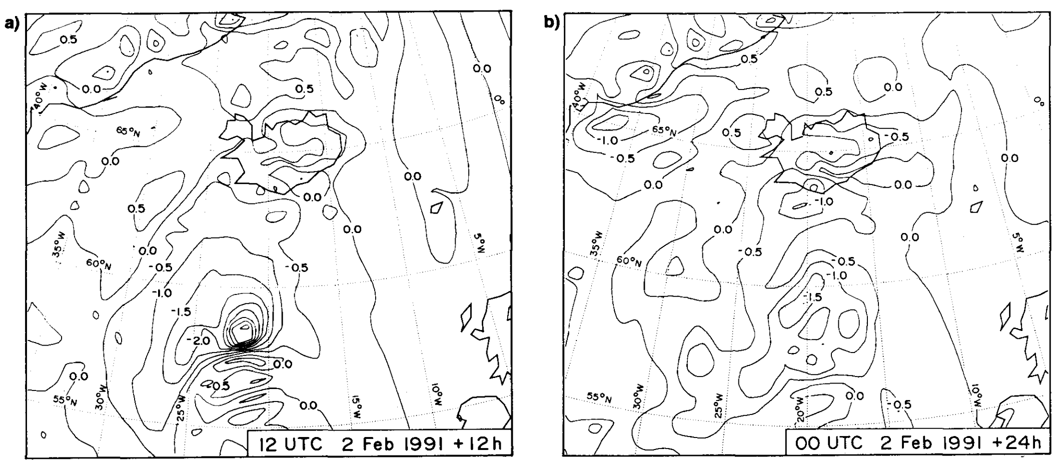

Fig. 11. Omega (Pa s^{-1}) at 500 hPa at 00 UTC 3 February 1991: (a) CONTROL, (b) RUN-00.

With reference to Figs. 2a and 5, we note that at this level the CONTROL run is up to 6° warmer in the warm sector, while it is correspondingly colder in the cold air to the north and west. The reason for this much stronger baroclinicity in the CONTROL run as compared to RUN00 is not obvious, but it evidently causes the cyclone in the former case to deepen more initially and hence to adopt a more westerly course.

The vertical velocity fields (Fig. 11) at 500 hPa at 00 UTC 3 February show distinctly the difference between the two simulations. Here we see in CONTROL a very strong and quite sharp updraft of almost -5 Pa s^{-1} above the surface low, while RUN00 has a less organized pattern with the largest negative omega values of almost -2.0 Pa s^{-1}. We also note that the updraft and the surface low (not shown) are shifted by about 100 km eastward. This trend continues and comparing PV between RUN00 and CONTROL 12 h later, we see from Figs. 8 and 12 that the 850–700 hPa PV maximum is shifted eastwards by about 200 km in RUN00 compared to CONTROL, as well as being somewhat weaker. Higher up, at 500–300 hPa the PV evolution is once again (see Subsection 3.4.2) quite similar to that of CONTROL (not shown).

Another run was conducted, starting at 06 UTC 2 February and termed RUN06. This run gave a result somewhat between that of RUN00 and CONTROL (Tables 2, 3). Apparently the initial state in this case contained some data, absent in RUN00, that caused the cyclone to deepen more initially (though not enough), thereby adopting a more westerly track. This in turn allowed the cyclone to interact with the upper level PV-anomaly in the early hours of 3 February. This argument is somewhat speculative and we are currently investigating methods to answer those questions more accurately, as explained below.

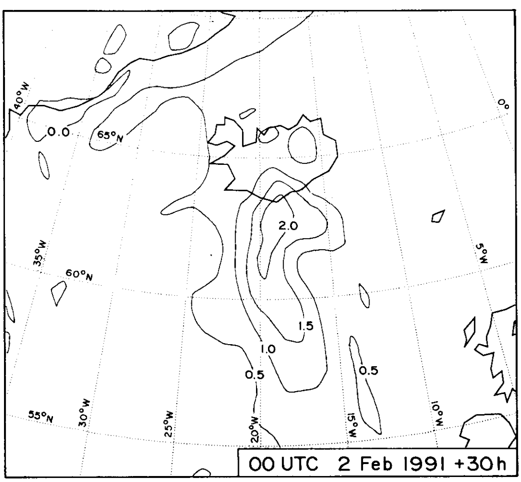

Fig. 12. As Fig. 8, but for RUN-00.

4. Summary and conclusions

The evolution of a record-breaking explosive cyclone that hit Iceland on 3 February 1991 has been investigated with the aid of meteorological data, as well as the HIRLAM model. Several simulations have been run, in order to study the role of different processes in the cyclone evolution. Based on the results, we are able to draw the following picture of the development of the cyclone.

- The initial stages of the cyclone's lifetime were characterized by exceptionally strong baroclinicity. Hence, a cyclone wave formed and was rapidly intensified as other processes interacted constructively with the wave.
- Latent heat release, probably linked to slantwise convection, played an active role in releasing energy in the warm, moist air near the cyclone center during the developing phase.
- An upper-level PV maximum which approached the surface cyclone from the southwest seems to be responsible for the final deepening stage of the cyclone.
- Latent heat release contributed about one third of the total deepening, which is less than what is found in other studies of comparable lows. This is attributed to the exceptional dry baroclinicity in this case.
- Surface fluxes played a negligible role during the 24 h where most of our studies were concentrated.
- Many operational models failed at the time, seemingly due to errors in mid-tropospheric temperature and humidity data. These errors precluded the early spin up of the cyclone wave, which set it on track for its meeting with the upper-level PV anomaly.

As a follow-up of the results presented here, we are presently looking at a new method to determine objectively the relative importance of different PV sources. This method has been described by Davis and Emanuel (1991) in a recent paper. Despite the non-linearity of Ertel's PV, the method seems capable of quantifying the contributions from different PV sources (anomalies) to the cyclone circulation. Through this method we expect to be able to answer more precisely questions raised in Section 3 regarding the apparent *merging* between the low-level cyclone and the upper-level PV anomaly. Results from this investigation will be reported under separate cover.

Although the cyclone studied here was in many ways exceptional, there is no doubt that the Icelandic region has more extratropical cyclone activity than almost any other region in the world. For this reason and due to the interesting effects of Greenland orography, SST gradients, etc., we believe that this region is particularly well suited for a comprehensive field experiment. This would preferably be concentrated on autumn and winter months and should be a combined observational, data assimilation and modelling effort.

5. Acknowledgments

This research has been supported financially by the Icelandic Council of Science. We wish to thank the former Director of the Icelandic Meteorological Office (IMO), Páll Bergthórsson and HIRLAM 2 project leader Dr. Nils Gustafsson, for their enthusiastic support. Also thanks to Rita Moi for analyzing the surface charts, Magnús M. Magnússon for allowing access to the computer of the Avalanche Division at IMO, to Gudmundur Hafsteinsson, Sigurdur Kristjánsson and Gudmundur Freyr Úlfarsson for assistance regarding computer graphics and to Pétur Örn Pétursson for drafting of figures.

REFERENCES

Breivik, L. A., Kristjánsson, J. E., Midtbø, K. H., Røsting, B. and Sunde, J. 1992. Simulations of the 1 January 1992 North Atlantic Storm. DNMI Technical Report no. 99, 69 pp. (Available from The Norwegian Meteorological Institute, P.O. Box 43 Blindern, N-0313 Oslo, Norway.)

Davis, C. A. and Emanuel, K. A. 1991. Potential vorticity diagnostics of cyclogenesis. *Mon. Wea. Rev.* **119**, 1929–1953.

Emanuel, K. A. 1985. Frontal circulations in the presence of small, moist symmetric instability. *J. Atmos. Sci.* **42**, 1061–1071.

Gíslason, K. 1991. Islands-orkanen den 3. februar 1991. *Vejret* **13**, 3–14, Danish Meteorological Society (in Danish).

Gustafsson, N. (ed.) 1993. Hirlam 2 final report. *Hirlam Technical Report* no. 9, 126 pp. (Available from Swedish Meteorological and Hydrological Institute, S-60176 Norrköping, Sweden.)

Gyakum, J. R. 1983. On the evolution of the QE II storm (I). Synoptic aspects. *Mon. Wea. Rev.* **111**, 1137–1155.

Hoskins, B. J., McIntyre, M. E. and Robertson, A. W. 1985. On the use and significance of isentropic potential vorticity maps. *Q. J. R. Meteorol. Soc.* **111**, 877–916.

Hoskins, B. J. and Berrisford, P. 1988. A potential vorticity perspective of the storm of 15–16 October 1987. *Weather* **43**, 122–129.

Kuo, Y.-H. and Reed, R. J. 1988. Numerical simulation of an explosively deepening cyclone in the eastern Pacific. *Mon. Wea. Rev.* **116**, 2081–2105.

Norris, J. and Young, M. V. 1991. Satellite photographs, 2 February 1991 at 1533 UTC. *Met. Mag.* **120**, 115–116.

Petterssen, S. 1956. *Weather analysis and forecasting*, 2nd edition, vol. I. Motion and motion systems. McGraw-Hill, 428 pp.

Reed, R. J., Simmons, A. J., Albright, M. A. and Undén, P. 1988. The rôle of latent heat release in explosive cyclogenesis: Three examples based on ECMWF operational forecasts. *Wea. Forecasting* **3**, 217–229.

Reed, R. J. and Simmons, A. J. 1991. Numerical simulations of an explosively deepening cyclone over the North Atlantic that was unaffected by concurrent surface energy fluxes. *Wea. Forecasting* **6**, 117–122.

Reed, R. J., Stoelinga, M. T. and Kuo, Y.-H. 1992. A model-aided study of the origin and evolution of the anomalously high potential vorticity in the inner region of a rapidly deepening marine cyclone. *Mon. Wea. Rev.* **120**, 893–913.

Roebber, P. J. 1989. On the statistical analysis of cyclone deepening rates. *Mon. Wea. Rev.* **117**, 2293–2298.

Shapiro, M. 1985. Dropwindsonde observations of an Icelandic low and a Greenland mountain-lee wave. *Mon. Wea. Rev.* **113**, 680–683.

Shapiro, M. A. and Keyser, D. 1990. Fronts, jet streams and the tropopause. In: *Extratropical cyclones. The Erik Palmén Memorial Volume* (ed. C. Newton and E. Holopainen), AMS, Boston, 167–191.

Shutts, G. J. 1990. A study of successful fine-mesh simulation. *Q. J. R. Meteorol. Soc.* **116**, 1315–1347.

Simmons, A. J. and Burridge, D. M. 1981. An energy and angular momentum conserving vertical finite-difference scheme and hybrid vertical coordinates. *Mon. Wea. Rev.* **109**, 758–766.

Stefánsson, U. 1961. *Hafid* (The Sea). Almenna Bókafélagid, Reykjavík, Iceland, 293 pp. (In Icelandic)

Stubbs, M. W. 1975. An unusually large fall of pressure. *Weather* **30**, 91–92.

Tryggvason, E. 1960. Rapid pressure variations in Iceland. *Mon. Wea. Rev.* **88**, 256.

Uccellini, L. W. 1990. Processes contributing to the rapid development of extratropical cyclones. In: *Extratropical cyclones*. The Erik Palmén Memorial Volume (ed. C. Newton and E. Holopainen), AMS, Boston, 81–105.

Vautard, R. 1990. Multiple weather regimes over the North Atlantic: Analysis of Precursors and Successors. *Mon. Wea. Rev.* **111**, 2056–2081.

Wallace, J. M. and Hobbs, P. V. 1977. *Atmospheric Science. An introductory survey*. Academic Press, 467 pp.